Available online at www.sciencedirect.com
SCIENCE DIRECT®
Bioorganic & Medicinal Chemistry 14 (2006) 6001–6011
Bioorganic & Medicinal Chemistry

Molecular docking study and development of an empirical binding free energy model for phosphodiesterase 4 inhibitors

Fernanda G. Oliveira,[a] Carlos M. R. Sant'Anna,[b] Ernesto R. Caffarena,[c] Laurent E. Dardenne[d] and Eliezer J. Barreiro[a,*]

[a]*LASSBio, Laboratório de Avaliação e Síntese de Substâncias Bioativas, Faculdade de Farmácia and Instituto de Química, Universidade Federal do Rio de Janeiro, PO Box 68006, Rio de Janeiro, RJ 21944-910, Brazil*
[b]*Departamento de Química, ICE, Universidade Federal Rural do Rio de Janeiro (UFRRJ), Seropédica, RJ 23851-970, Brazil*
[c]*Programa de Computação Científica—Fundação Oswaldo Cruz (FIOCRUZ/MS)—Manguinhos, RJ 21045-900, Brazil*
[d]*Laboratório Nacional de Computação Científica—LNCC/MCT, Quitandinha, Petrópolis, RJ 25651-075, Brazil*

Received 8 November 2005; revised 10 May 2006; accepted 10 May 2006
Available online 14 July 2006

Abstract—In the present work, several computational methodologies were combined to develop a model for the prediction of PDE4B inhibitors' activity. The adequacy of applying the ligand docking approach, keeping the enzyme rigid, to the study of a series of PDE4 inhibitors was confirmed by a previous molecular dynamics analysis of the complete enzyme. An exhaustive docking procedure was performed to identify the most probable binding modes of the ligands to the enzyme, including the active site metal ions and the surrounding structural water molecules. The enzyme–inhibitor interaction enthalpies, refined by using the semiempirical molecular orbital approach, were combined with calculated solvation free energies and entropy considerations in an empirical free energy model that enabled the calculation of binding free energies that correlated very well with experimentally derived binding free energies. Our results indicate that both the inclusion of the structural water molecules close to the ions in the binding site and the use of a free energy model with a quadratic dependency on the ligand free energy of solvation are important aspects to be considered for molecular docking investigations involving the PDE4 enzyme family.

1. Introduction

The cyclic 3′–5′ nucleotides adenosine (AMPc) and guanosine (GMPc) are second messengers that play a key role in many physiological processes by transducing the signals of a variety of extracellular mediators. These nucleotides are inactivated by a superfamily of enzymes known as phosphodiesterases (PDE). At present, at least 11 families of PDE isoenzymes have been described (PDE1–11), being characterized by different substrate specificity (cAMP or cGMP), inhibition, substrate requirements, gene sequence, and tissue distribution.[1,2] The PDE family shares the same general structure, a conserved catalytic domain of about 300 amino acids with a 25% sequence similarity and a N-terminal regulatory domain.[3]

The PDE4 isoform is responsible for the metabolism of cAMP in pro-inflammatory and immune cells, suggesting a potential application in the therapeutics of inflammatory and immune disorders like asthma and chronic obstructive pulmonary disease (COPD).[1,4] The PDE4 isoform is encoded by four distinct genes (A, B, C, and D), for which a number of splice variants have been described sharing identical catalytic and C-terminal domains and with modifications in the sequence at the N-terminal end of the protein.

PDE4 inhibitors have been found to interact through the same enzyme binding site resulting in different affinities, depending on the protein conformation, as exemplified for the inhibitor rolipram.[5–7] Rolipram binds to the high-affinity and low-affinity binding states of the protein with K_i values of 5–10 nM and 350–400 nM, respectively. The presence of both the N-terminal domain and the catalytic domain is essential for the high-affinity binding state, while the low-affinity binding state requires only the presence of the catalytic domain.[8] It has been suggested that agents displaying potent

Keywords: Phosphodiesterases; Molecular modeling; Molecular docking; Empirical free energy model; Semiempirical calculations.
* Corresponding author. Tel./fax: +55 21 25 62 66 44; e-mail: ejb@pharma.ufrj.br

0968-0896/$ - see front matter © 2006 Elsevier Ltd. All rights reserved.
doi:10.1016/j.bmc.2006.05.017

catalytic site inhibitory activity with a reduced activity at high-affinity binding state of PDE4 would have good anti-inflammatory activity, with a decreased potential to induce side effects such as emesis, nausea,[9–11] headache, psychotropic activity,[11–14] and gastric alterations.[11]

The factors that determine the conformation of PDE4 are not fully understood, although it is known that post-translational modification and membrane association have marked pharmacological effects.[15–17] Another factor that could influence the conformation is the presence of two divalent metal ions at the bottom of the enzyme active site, observed in the crystal structure of PDE4B, which are involved in both cAMP binding and hydrolysis.[18,19] There are suggestions that the two conformations of PDE4 are a consequence of the binding to a metal ion cofactor, such as Mg^{2+}, eliciting the high-affinity and productive cAMP binding to the active site.[18,20,21]

The prediction and understanding of the detailed enzyme inhibition process may help in the development of drugs with increased therapeutic benefits, but the complexity of the process as a whole presents many difficulties for achieving this goal. The theoretical investigation of the receptor–ligand molecular recognition process by molecular docking methodologies has two key aspects. The first one is the correct prediction of the ligand–receptor binding mode, which involves a search on the receptor–ligand potential energy landscape considering the ligand conformational degrees of freedom and usually assuming a rigid receptor conformation. Methods to improve docking performance have been proposed, such as the use of X-ray data to focus the sampling on specific regions[22] and the use of a local rigid optimization followed by a final full minimization on the energy minima.[23]

The second key aspect is the right prediction of the binding free energies associated to the predicted ligand–receptor binding mode. Methodologies which use computationally expensive conformational sampling-based strategies (e.g., free energy perturbations,[24,25] linear interaction energies' approximations[26–28]) can accurately estimate binding free energies but are very time consuming and, consequently, appropriate only for studies involving few ligands. A semiempirical quantum mechanics-based scoring function was developed to evaluate protein–ligand binding free energies, which were used to score known metal-containing protein–ligand poses.[29] Simplified and computationally viable scoring methods were proposed to semiquantitatively estimate binding affinities,[30] based on the assumption that the binding free energies can be partitioned in terms of individual interactions that are additive and independent of each other. Programs such as FlexX[31] and ChemScore[32] use empirical terms to estimate binding free energies. The coefficients of each term are obtained by performing a regression on a set of receptor–ligand complexes with known experimental binding affinities. Despite the theoretical drawbacks that have been pointed out on this approach,[33] these empirical methods have provided useful information. In a similar theoretical approach, the enzyme inhibition process can be split up in a series of enthalpy and entropy factors, which include terms that can be evaluated separately, such as the energies associated with the inhibitor binding to the enzyme, desolvation, and restrictions on the inhibitor molecule movements upon binding, including internal rotations.[34,35]

PDE4 inhibitor development presents a promising approach to the treatment of inflammatory diseases. As an initial step toward this objective, we present here the implementation of a theoretical methodology for the analysis of the PDE4-inhibitors interactions. The methodology included a previous detailed evaluation of the molecular flexibility of the complete enzyme through a molecular dynamics (MD) simulation in order to verify the adequacy of using a rigid protein in a docking study of selected PDE4 inhibitors. The MD calculations were performed on PDE4D and PDE4B isoforms. PDE4D is the isoform co-crystallized with rolipram[3] and it was used to verify the docking performance for identifying the bioactive orientation of a PDE4 inhibitor, whereas PDE4B was the isoform chosen for the development of our model. This model was based on an extensive docking search procedure on a series of PDE4 inhibitors from the literature[36] including the structural water molecules, and the metal ions of the active site. The semiempirical molecular orbital method was used to refine the binding enthalpy for the best scored orientations of the ligand dataset. This method was applied to enzyme/ligand complex models containing amino acid residues, water molecules and metallic ions observed in the enzyme active site to include in the enthalpy evaluation the influence of interaction terms that are generally not considered by the classical approach, such as charge-transfer interactions between the metallic ions and the ligand and π and T-stacking interactions. The inclusion of dispersive and charge-transfer interactions obtained by quantum methods for the adequate evaluation of intermolecular energetics and optimal geometries involving aromatic molecular systems is well documented in the literature.[37–41] The calculated enzyme–inhibitor interaction enthalpies, together with calculated solvation energies and entropy considerations, were used to construct, through a multiple regression approach, an empirical model that allowed the prediction of free energies of binding, which correlate quite well with the inhibitory profile of the PDE4 inhibitors.

2. Results and discussion

The present study was divided in the following phases: (i) a molecular dynamics analysis of the active site conformational flexibility of the isoforms PDE4B and PDE4D to verify the adequacy of using a rigid protein in docking studies; (ii) a conformational docking study using the inhibitor rolipram in the PDE4D active site to investigate the importance of structural active site water molecules; (iii) a conformational docking study to investigate the different binding modes of a set of

ligands inside the PDE4B enzyme; (iv) investigation of the distinct ligand binding modes with a quantum semi-empirical method instead of a classical molecular force field; (v) development of an empirical model for the prediction of free energies of binding of the PDE4 ligands. The details about each procedure are described in the methodology section.

A set of 10 ligands was selected from the work of Dal Piaz et al.[36] (Chart 1). These compounds were chosen because they present an adequate structural variability with a large activity range. Additionally, they were all evaluated according to the same pharmacological protocol, with purified PDE4 extracted from the ventricular tissue of guinea pigs using cAMP as the substrate, allowing a direct comparison of the measured biologic data. The chosen dataset presented the advantage of containing the PDE4 selective inhibitor rolipram, whose X-ray structure co-crystallized with PDE4 is known.

We focused our attention to the PDE4 isoforms B and D. These isoforms are the only ones that have their crystallographic structures deposited in the Protein Data Bank. The construction of our model was based on the PDE4B isoform because the experimental data were obtained with an enzyme purified from the ventricular tissue,[36] a tissue where PDE4B mRNA is more expressed than PDE4D mRNA.[42]

2.1. Molecular dynamics analysis of the enzyme active site conformational flexibility

The similarity between the amino acid sequences of the catalytic sites of both enzymes—PDE4B and PDE4D—is 85%. When calculating the root mean square deviation (rmsd) between the active site α-carbon atoms of both structures, we obtained a value of 0.33 Å (3.3×10^{-11} m). This result indicates that the PDE4D active site three-dimensional structure, even co-crystallized with rolipram, presents a slight difference when compared to the PDE4B isoform (crystallized without any ligand), which is suggestive that local ligand induced-fit effects to PDE4 are not very relevant, at least in the crystalline state. To evaluate the extension of this hypothesis to dynamic conditions closer to those of the biophase, one-nanosecond MD simulations of both enzymes, without the inhibitor in the active site, were performed separately. During the analyzed trajectory, after a stabilization period of 500 ps, we observed only a minor variation of active site α-carbon root mean square fluctuation (rmsf) values.

Figure 1 shows that the backbone C_α rmsf fluctuations (taking the crystallographic structure as the reference) for the active site residues are less than 1.0 Å in PDE4B simulation, except for the α-carbon atom of Met431, which is more exposed to solvent and, consequently, presents greater mobility. Within the active site, only

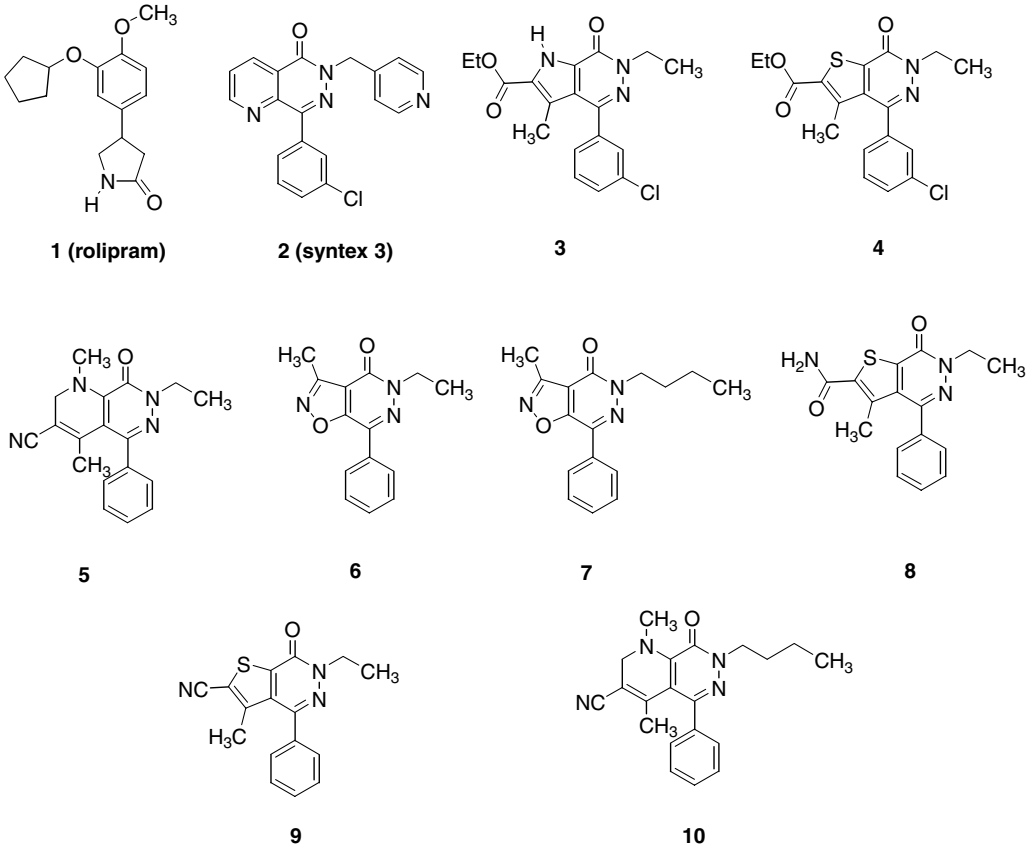

Chart 1. PDE4 ligands used in this work.[36]

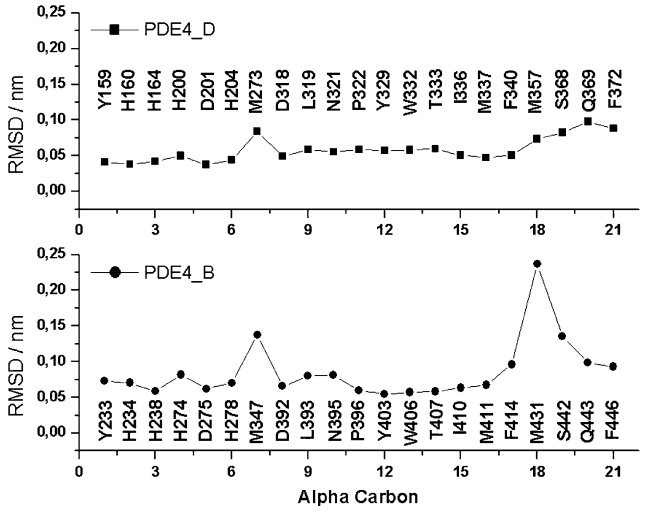

Figure 1. Molecular dynamics rmsd fluctuation values of the active site α-carbon atoms of the PDE4D and PDB4B, with crystallographic structures as reference.

the Met347 residue presented a rmsf value superior to 1.0 Å. Also, the shapes of both curves (PDE4B and PDE4D) look the same, indicating possible similar dynamical behavior. The small conformational variation of the PDE4D active site α-carbon atoms suggests that, even in dynamical conditions, the site remains quite rigid. The MD simulation indicates that the two enzyme isoforms present low conformational flexibility at the active site region. This fact is in agreement with the experimental observation that the catalytic domain of PDE4 folds into a compact structure composed of rigid α-helices[18] and to the small rmsd values between the α-carbons of the X-ray structures of PDE4B2B and of PDE4D co-crystallized with rolipram.[3] This fact justifies, to some extent, the adequacy of using the rigid protein approximation in a ligand/enzyme docking study.

2.2. Docking analysis

The docking results show that the best *R*-rolipram binding mode inside the active site of PDE4D without the water molecules presents a rmsd = 4.5 Å relative to the crystallographic conformation[3] (Fig. 2A). In this conformation, *R*-rolipram is interacting directly with the divalent metal ions. Investigation of the second most stable binding mode revealed a conformation closer to the experimental one, with a rmsd = 3.7 Å (Fig. 2B). When we considered the five water molecules in the vicinity of the metallic site as part of the enzyme, the best docked rolipram conformation exhibited a rmsd = 3.4 Å relative to the experimental one (Fig. 2C). This result suggests that these five water molecules should be considered in docking studies involving the PDE4 active site in order to obtain better structures. A previous published analysis of the PDE4 binding site made by Gratteri et al. showed that the five water molecules considered in this work are in a very favorable interaction area of the PDE4 active site, corroborating our choice to consider them as part of the PDE4 active site. Docking results obtained by Gratteri et al. also showed that the explicit consideration of only two of these five water molecules improves the performance of their docking experiments. In our opinion, the remaining water molecules should be included during the docking procedure because a considerable amount of energy will probably be necessary for a ligand to displace them from their positions since they are interacting tightly with the metal ions. Some of these water molecules are also hydrogen bonded to amino acids closer to the metallic site.

The main difference observed between the best docked *R*-rolipram conformation and the experimental one is the orientation of the pyrrolidinone ring. However, Xu et al.[19] have recently shown that the pyrrolidinone ring of rolipram, in complex with the PDE4B isoform, could adopt two different orientations, one corresponding to the PDE4D crystallographic orientation[3] and the other similar to our results obtained including the structural water molecules (Fig. 2C).

In Table 1, a summary of the 120 independent docking runs for each ligand is shown. Considering the results for all ligands, we found a minimum of 3 (ligand **9**) and a maximum of 12 (ligand **4**) distinct binding modes.

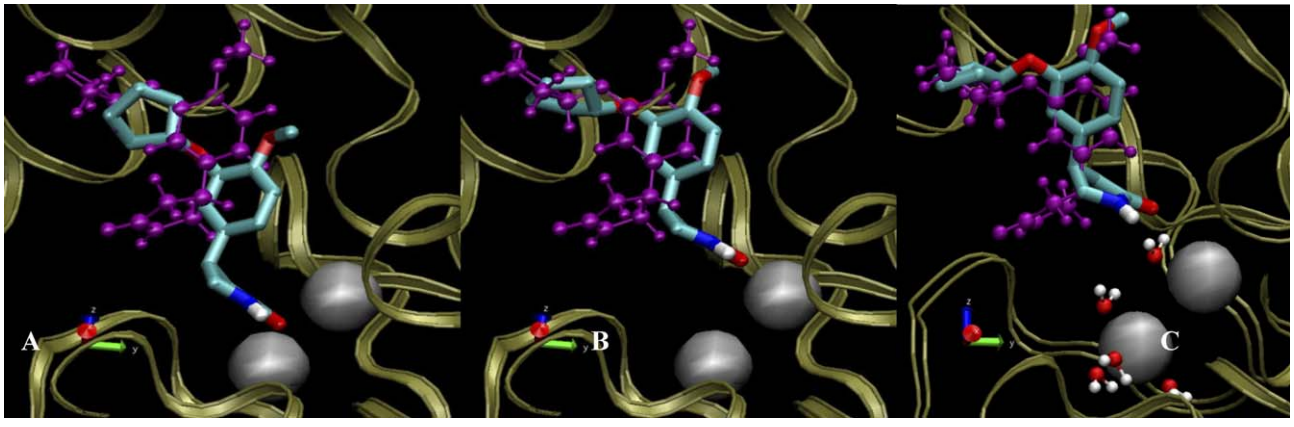

Figure 2. PDE4D2 docked *R*-rolipram binding modes. (A) and (B) Docking without the water molecules associated with the active site metals (gray spheres). (A) is the most stable binding mode and (B), the second one. (C) The most stable binding mode found by docking with the five active site water molecules. The crystallographic conformation of *R*-rolipram is presented for comparison (magenta ball and stick structure).

Table 1. Ligand binding modes obtained by the docking methodology

Ligand	Number of binding modes[a]	Min (max) energy[b] (kJ/mol)	Min (max) rmsd[c] (Å)
1 (*R*-rolipram)	4	−41.42 (−38.79)	2.29 (4.74)
2 (syntex3)	11	−43.30 (−38.03)	4.73 (10.93)
3	11	−44.89 (−37.15)	2.04 (8.44)
4	12	−44.64 (−37.66)	2.34 (9.73)
5	5	−43.56 (−38.70)	4.72 (5.22)
6	8	−33.89 (−27.28)	3.39 (10.97)
7	11	−39.96 (−35.19)	4.10 (9.68)
8	4	−39.96 (−38.37)	4.72 (5.40)
9	3	−39.08 (−37.45)	4.58 (4.75)
10	6	−48.03 (−48.89)	5.09 (10.63)

[a] Number of ligand binding modes based on the result of 120 independent docking runs with the final conformations clustered by their root-mean-square positional deviation (⩽2.0 Å criterion, see text).
[b] Minimum and maximum interaction energy of the representative conformations of the ligand binding modes.
[c] Minimum and maximum rmsd of the representative conformations of the ligand binding modes relative to the best ligand energy binding mode/conformation.

The representative conformations of the different ligand binding modes have rmsd values ranging from 2.04 to 10.97 Å relative to the best representative conformation/binding mode found. On the other hand, it is interesting to observe that the representative conformations of the distinct binding modes have a maximum energy difference of 7.74 kJ/mol (ligand **3**) and a minimum of 1.60 kJ/mol (ligand **8**). These results show that a wide ligand conformational search space was investigated but also that the distinct ligand binding modes have similar binding energies and therefore it is very difficult to recognize the bioactive one.

2.3. Analysis of the complexes between PDE4 and the ligands calculated by the semiempirical method

After the docking procedure, all complexes were completely energy minimized with the Tripos forcefield as implemented in Sybyl6.8 (Tripos, Inc.), but the correlation between the most favorable interaction energies obtained by this approach and the IC_{50} data were very poor ($r^2 = 0.15$, SD = 3.77, $F = 0.26$). A possible reason for this weak result is a poor description, by the classical force field, of some interaction energy terms in the PDE4–ligand complex, which prompted us to use a quantum mechanical method to reevaluate the energetics of ligand–PDE4 complexes formation.

The representative conformations of the binding modes **1** to **6** obtained for each ligand from the docking study were then used as the initial geometries for semiempirical molecular orbital calculations. For each conformation, only the amino acids with direct contacts with the ligand were chosen for the construction of the active site model, which always included the two metallic ions and the five water molecules. In a few cases, the ligand moved out partially or completely from the active site model after optimization. Table 2 presents the interaction enthalpy calculated in accordance with Eq. 2 (see Section 4) for each ligand that remained within the active site.

Table 2. Semiempirical interaction enthalpy for the ligands inside the PDE4B2B active site model

Ligand	IC_{50}[a] (μM)	Binding mode[b]	ΔH_{int}[c] (kJ/mol)
1 (*R*-rolipram)	0.32	**1**	**−118.53**
		3	−89.08
		4	−82.01
2 (syntex3)	0.056	1	−73.97
		2	−42.97
		4	−62.26
		5	−49.37
		6	**−113.18**
3	0.6	1	−75.65
		2	**−109.08**
		3	−104.31
		4	−88.41
		5	−92.93
		6	−96.15
4	0.9	1	−59.12
		2	**−113.47**
		3	−71.25
		4	−101.17
		5	−44.69
5	1.1	1	−87.82
		2	−66.36
		3	−85.77
		4	**−94.14**
		5	−86.23
6	9	1	−52.3
		2	−42.76
		3	−47.11
		4	**−66.78**
		5	−63.89
7	6	1	−57.78
		2	−42.8
		3	−74.52
		4	−77.74
		5	**−80.21**
		6	−63.55
8	3	1	−105.56
		2	−91
		4	**−110.71**
9	4	**1**	**−69.37**
10	2	**1**	−115.65
		2	−66.27
		3	**−118.95**
		5	−118.53

[a] Dal Piaz et al.[36]
[b] Groups of geometries from the docking results.
[c] Obtained from Eq. 2. Bold numbers indicate the most stable complex.

Huai et al.[3] have subdivided the PDE4D2 active site in three subsites according to interactions with different parts of the co-crystallized inhibitor rolipram. We observed that syntex3 (ligand **2**), the most active compound of the ligand series, occupies all three subsites at least partially: in subsite 1, the chloro-phenyl group makes π and T stacking interactions with Phe446 (centroid–centroid distance = 4.15 Å) and Phe 414 (centroid–centroid distance = 4.17 Å), respectively (Fig. 3). This subsite, composed by residues Met411, Met431, Phe446, and Phe414, is essentially hydrophobic, but contains at its bottom the hydroxyl group of Ser442. As this residue is not conserved among the PDE families, interactions with it can be explored for the development of selective inhibitors. Subsite 2 is occupied by the

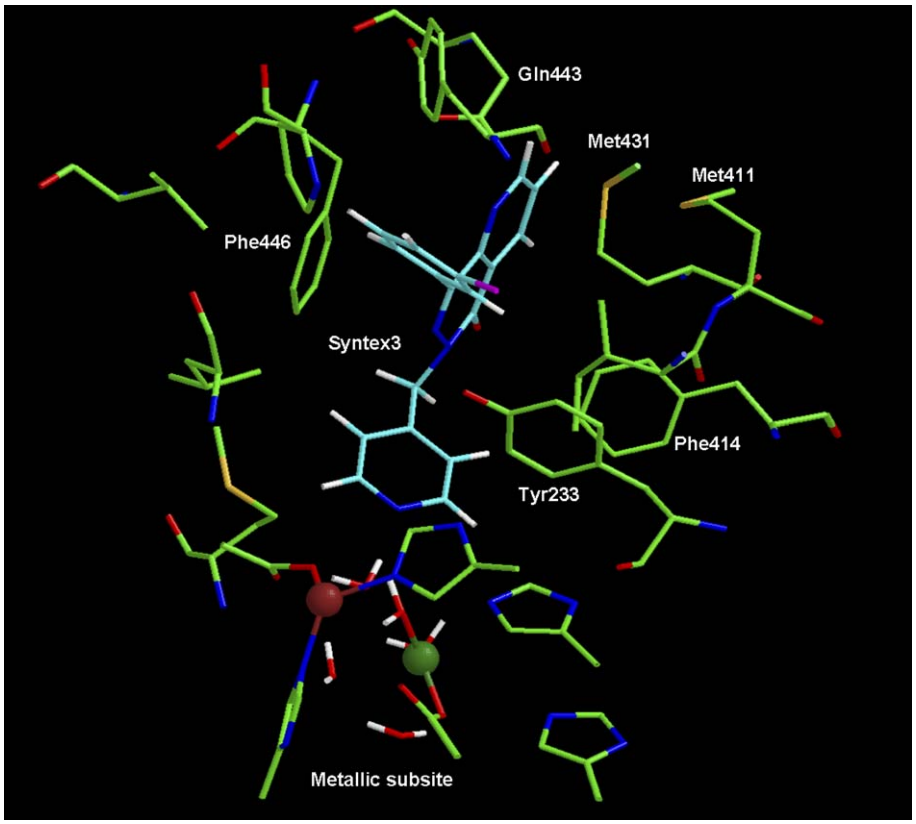

Figure 3. PM3 optimized best docked conformation of syntex3 inside PDE4B active site. Hydrogen atoms of amino acid residues were omitted for clarity. Color code: C (amino acid), green; C (ligand), cyan; N, blue; O, red; H, white; S, yellow; Cl, magenta; Zn, brown; Mg, dark green.

fused rings of syntex3 (**2**). The pyridine ring occupies subsite 3, where it interacts with non-polar groups at the same time that its nitrogen atom interacts with the Mg^{2+} ion by means of a water molecule.

Gln443 was found to interact with all ligands, with the exception of ligand **6**, which interacts with Tyr233. As described by Huai et al.[3], Gln443 is a key residue for selective inhibition of PDE4. Although it is a conserved residue in the PDE families, this residue is found in different conformations depending on the interacting amino acid residue. The interaction between Gln443 and Tyr403 is apparently essential for the selectivity of rolipram, because a serine residue replaces Tyr403 in PDE7, which is not inhibited by rolipram.

The subsite 1 is composed by the side chains of two phenylalanines, Phe414 and Phe446, which are in suitable positions to make π and T stacking interactions with aromatic groups of the ligands. For the most stable conformation of all molecules of our ligand data bank, it was observed that this site was occupied by an aromatic system, with the exception of ligand **7**, which inserted a butyl group at this site. Inhibitors containing groups with high electron density pointed these groups toward the metallic ions, where they interacted with the water molecules located at this subsite. In the case of compounds **9** and **10**, for example, a cyano group interacted with the water molecules but, at the same time, these compounds were not able to interact properly with residues of the subsite 3. It is interesting to observe that compounds **6** and **7**, which have the lowest activities in the series, did not interact with the water molecules located in the subsite containing metallic ions.

2.4. Calculated interaction enthalpy versus enzyme inhibition

Compared with the correlation obtained with the molecular mechanics method, the correlation between the semiempirical interaction enthalpies, for the most stable complex identified for each ligand, and the corresponding experimental IC_{50} values[36] has improved, but it was only moderate ($r^2 = 0.68$, SD = 2.92). It was observed, for example, that rolipram (ligand **1**) presented a more favorable interaction enthalpy than the most active compound of the series, syntex3 (ligand **2**). This result suggested that, although important, the interaction enthalpy by itself was not sufficient to produce a quantitative PDE4 inhibition model. Other phenomena associated with the enzyme inhibition must play important roles and they should be considered in order to improve the model.

2.5. The free energy model

Consideration of a linear dependence on ΔG_{solv} ($n = 1$) in Eq. 3 (see Section 4 below) resulted in a weak correlation between calculated and experimental ΔG values ($r^2 = 0.54$, SD = 0.74, and $F = 2.37$), when a multiple

Table 3. Contributing values of Eq. 1, calculated free energy changes, and experimental K_i-derived free energy changes

Molecule	ΔH_{int}[a] (kJ/mol)	N_{RB}[b]	ΔG_{solv}[c] (kJ/mol)	ΔG[d] (kJ/mol)	ΔG_{exp}[e] (kJ/mol)
1 (*R*-rolipram)	−118.53	4	−47.70	−50.28	−49.66
2 (syntex3)	−113.18	2	−40.96	−52.64	−53.97
3	−109.08	3	−34.94	−49.55	−48.12
4	−113.43	4	−26.74	−45.64	−47.11
5	−94.14	1	−23.14	−46.19	−46.61
6	−66.78	1	−22.68	−42.66	−41.38
7	−80.21	2	−21.00	−41.76	−42.38
8	−110.71	3	−68.53	−44.07	−44.10
9	−69.37	2	−25.31	−42.79	−43.39
10	−118.95	3	−23.64	−46.33	−45.10

[a] Calculated with Eq. 2.
[b] Determined by analysis of optimized complex structures.
[c] Calculated with the SM5.4 model.[64]
[d] Calculated with Eq. 1.
[e] Calculated as $RT\ln K_i$ from the IC_{50} results of Dal Piaz et al.[36]

regression model was applied to the relevant quantities associated with the PDE4 inhibitors, compiled in Table 3.

However, the inclusion of a quadratic dependence of ΔG on ΔG_{solv} produced a much better correlation.

$$\Delta G = 0.012(\Delta G_{solv} + 44.95)^2 + 0.12\Delta H_{int} + 1.55N_{RB} - 42.38 \quad (1)$$

with very good statistical parameters, $r^2 = 0.92$, SD = 1.43, and $F = 14.11$. This suggests that the inclusion of a quadratic solvation term and the inclusion of the entropic loss term associated with bond rotation restriction are important to predict the free energy changes related to the PDE4 inhibitor binding (Fig. 4).

It is worth noting that the value of c_4 that emerged from the multiple regression model is similar to the lower limit (1.50 kJ/mol) of the entropic loss range for each rotor restricted during substrate–enzyme binding, estimated by Searle et al.[35] The parabolic dependence of the solvation free energy is indicative that a high hydrophilicity and a high hydrophobicity will be deleterious to the inhibition of the PDE4 enzyme. Wang et al.[34] obtained good results when using a water solubility dependent quadratic term for a system where the ligands interacted with their receptor at the lipid phase. We believe that in the current case, in which the experimental data were obtained in the aqueous phase, the ligand ΔG_{solv} quadratic dependence can reflect the dual hydrophilic/hydrophobic character of the enzyme active site, as it can be clearly seen for syntex3 in Figure 3. In other words, a good PDE4 ligand has to be able to favorably interact with a hydrophilic environment located at the metal ions subsite and, at the same time, to favorably interact with the hydrophobic active site regions.

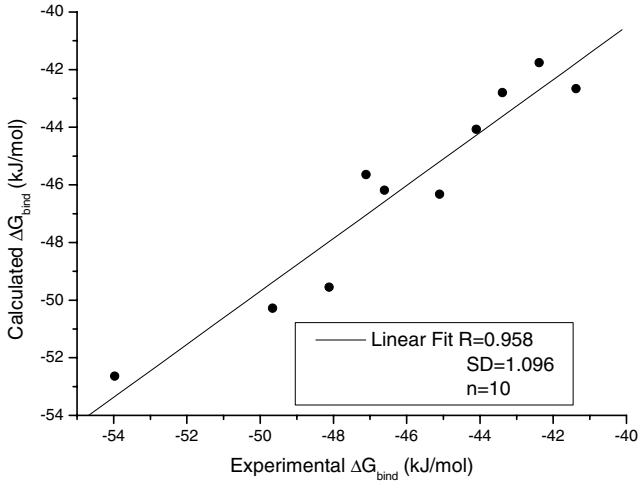

Figure 4. Correlation between experimental and calculated binding free energies.

3. Conclusions

In the present work, several important molecular docking aspects for the study of the PDE4B inhibition were investigated. A MD simulation of the PDE4B and PDE4D enzymes (with no ligands) showed no major conformational changes in their active sites, which, in addition to low values of root mean square deviation, indicate that local ligand induced-fit effects to PDE4 are probably not very relevant. This result supports the application of a ligand docking approach considering the enzyme rigid by validating the methodology and preventing our results against methodological artifacts.[43] However, it is expected that large scale PDE4 movements occur associated with a conformational switching between the low-affinity rolipram binding site conformation and the high-affinity rolipram binding site conformation. This conformational switching of the catalytic unit is poorly understood and can depend on whether the enzyme has a bound Mg^{2+} in its active site and/or it is associated with interactions of the PDE4 catalytic unit with other proteins or N-terminal regulatory regions.[44]

The docking results of *R*-rolipram interacting with the PDE4D enzyme showed that it is important to explicitly include the structural water molecules present in the proximity of the enzyme metallic site in order to better represent the distinct ligand binding modes. The development of an empirical free energy model, inspired in the work of Wang et al.,[34] resulted in a very good

correlation ($r^2 = 0.92$) between experimental[36] and theoretical data.

A key aspect associated with the developed free energy model was the use of a quadratic dependence on the ligand free energy of solvation, which probably reflects the dual hydrophilic/hydrophobic character of the PDE4 active site. Another important feature was the use of a quantum semiempirical molecular orbital methodology to calculate the enzyme/ligand interaction enthalpies, which permitted a more reliable evaluation of relevant intermolecular interactions such as T and π stacking between aromatic groups, and charge-transfer interactions between the metal ions and the ligand and the enzyme which are also expected to be present in the PDE4 family active site. As an alternative approach for future studies, with a considerable low computational cost, it is possible to use more sophisticated molecular mechanics forcefields grounded in quantum chemistry[45–47] which include polarization, dispersion, and charge-transfer effects, in order to improve inhibitor–enzymes interactions.

It is important to note that almost all studied ligands have an aromatic group involved in stacking interactions with the Phe414 and Phe446 residues present in the PDE4 subsite 1. Accordingly, the absence of π and T stacking interactions in previous docking results accomplished with the classical approach[48] might be attributed not only to the absence of an adequate methodology for the evaluation of such interactions, but also to the lack of representation of the structural water molecules close to the metallic subsite, which influence the position of the ligand inside the active site. In fact, investigation into the available crystallographic structures uploaded to the PDB revealed that almost all neutral ligands do not interact directly with the metal ions. The only exception observed was the inhibitor zardaverine, which interacts with the PD4D zinc ion by means of its carbonyl group.[49] Charged ligands, such as the enzyme substrate, can displace some water molecules and interact directly with the metals.

Due to the conservative character of the active site region among enzymes belonging to the PDE4 family, we consider that the discussion developed in this work can be useful for molecular docking studies involving other PDE4 isoforms. Finally, it is clear that the methodology developed in this work suffers from limitations associated with the approximations inherent to simplified empirical models. In this sense, we think that the inclusion of explicit water molecules and full flexible enzyme/inhibitor MD is the natural (but more computationally expensive) next step for a better investigation of the inhibition profile.

4. Experimental methodology

4.1. Molecular dynamics

The MD approach is a suitable computational technique to study the flexibility of macromolecules. To analyze the conformational stability and rigidity of the enzyme active site, MD simulations of the PDE4B (PDB code: 1F0J) and PDE4D (PDB code: 1OYN) isoforms were performed in the Gibbs statistical ensemble using the GROMACS (version 3.2) software.[50,51] The amino acids 490–495, constituting a discontinuous isolated α-helix and with a conformation that is probably a crystallographic artifact, along with two arsenic atoms (artifacts from the crystal preparation) present in the PDE4B file (1F0J) were excluded from all calculations. Simulations were carried out using the OPLS_AA[52] force field and the TIP3P[53] water model accounting for the solvent. Proper dihedral angles were parameterized using the Ryckaert–Belleman representation[54] and bond lengths were kept fixed throughout the simulation by the LINCS[55] constraint algorithm. The crystallographic structures of PDE4B and PDE4D were immersed in orthogonal boxes of volume $65 \times 65 \times 75$ Å^3 and solvated with 9795 and 9752 water molecules, respectively. In order to make both systems electroneutral, 18 and 16 sodium counter ions were added for the PDE4B and PDE4D systems, respectively. Periodic boundary conditions were used throughout the simulations. Both systems were energetically optimized with 100 steps of the steepest descent energy minimization, followed by 100 steps of conjugate gradient method in order to eliminate residual geometrical strains and to accommodate the molecular structures to the force field parameters. The simulations were carried out in an AMD Athlon 2.6 GHz computer, integrating the Newton's equations of motion using the Leap-frog algorithm[56] with an integration step of 2 fs, cutoff radii for non-bonded interactions of 16 Å and 14 Å, for Coulomb and van der Waals terms, respectively. The system was weakly coupled to a heat bath and a hydrostatic bath to work in the NPT ensemble at $T = 300$ K and $P = 1$ atm (1.013×10^5 Pa) with coupling constants of 0.1 ps and 0.5 ps, respectively. MD trajectory collection was initiated after 1 ns of dynamics to guarantee an equilibrated evolution. Throughout the first 500 ps, only water molecules were allowed to move and, for the next 500 ps of the equilibration stage, no molecular restraints were applied. Production trajectories were collected during 1 ns with a periodicity of 1 ps.

4.2. Docking

The different ligand binding modes of the PDE4B enzyme were investigated by using a docking methodology implemented in the AutoDock program (version 3.0). A Lamarckian Genetic Algorithm[57] with an initial population size of 100 random individuals was used with probabilities of 0.02 and 0.8 for gene-mutation and crossover operators, respectively. The pseudo-Solis and Wets local search method was used with a probability of 0.06 to be applied on an individual in the population. The docking calculations were performed by using a grid map of $60 \times 60 \times 60$ points centered in the enzyme active site, with 0.375 Å grid-point spacing. The MMFF94[58] partial atomic charge parameter set was used for all ligands. For each ligand we performed flexible ligand docking calculations using three different initial conformations (obtained by manual docking). For

each initial ligand conformation we performed 40 independent docking runs with a maximum number of 2.5×10^6 energy evaluations per run. Therefore, for each ligand we obtained 120 binding conformations, which were clustered by their root-mean-square positional deviation (rmsd), by using a homemade program following the next steps:

(1) The N final conformations were ordered according to their total energy (intra + intermolecular) and, the first conformation (with the lowest energy) was considered as the representative member of the first cluster (C_1). All conformations with rmsd $\leqslant$2.0 Å relative to this typical conformation were associated with cluster C_1.
(2) The most stable conformation, not associated previously with any cluster, was designed as the representative conformation of the cluster C_{m+1} (typical of the $m + 1$ binding mode). All remaining conformations, not designed yet to any cluster, with rmsd $\leqslant$2.0 Å relative to this conformation were associated with the C_{m+1} cluster.
(3) Step 2 is repeated until all the N final conformations were attributed to some specific cluster.

The docking methodology was first tested for the rolipram molecule considering two distinct receptor situations: (i) the receptor with the two divalent metal ions (Zn^{2+} and Mg^{2+}) located in the active site without considering the water molecules in the proximity; and (ii) the receptor with the two divalent metal ions and five water molecules with a distance $\leqslant$3.0 Å from any of the two metal ions. Based on the obtained results, the docking methodology was applied to the remaining ligand molecules including the five water molecules close to the divalent metal ions as part of the active site.

4.3. Semiempirical calculations

The molecules of the inhibitor dataset and the side chains of some of PDE4B active site residues contain aromatic rings, suggesting the possibility of aromatic–aromatic interactions. This kind of interaction was recently analyzed with state-of-the-art electronic structure methods, which demonstrated the complexity of the phenomenon, with participation of electrostatic and dispersion contributions, particularly when there are substituents on the aromatic rings.[59] The inclusion of electronic effects, at the quantum semiempirical molecular level, is expected to result in better geometries and calculated energies than those obtained with a classical force field parameterization. Thus, the representative receptor/ligand binding modes obtained by the docking methodology were subjected to geometry optimizations at the quantum semiempirical molecular orbital level. These geometry optimizations were performed with the MOPAC 6.0 program[60] using the PM3 Hamiltonian.[61] All geometries were optimized with the eigenvector following routine[62] to a gradient norm <2.0 kJ/(Å or rad). For the semiempirical calculations, the enzyme/ligand complexes were simplified by selecting only the amino acid residues capable of interacting directly with the ligand molecules, as observed in the previously docked structures. Both metal cations and the five water molecules observed in their vicinity in the crystal structure[18] were also included in all model complexes together with the side chains of the amino acid residues that compose the metallic subsite. The truncated bonds were saturated with hydrogen atoms added with Sybyl 6.8 program [Tripos Software, Inc.]. The positions of delta and gamma carbon atoms of the metallic subsite amino acid side chains and of the peptidic bonds of the remaining amino acid residues were kept fixed during the geometry optimization procedure.

The interaction enthalpy was determined by the following equation,

$$\Delta H_{\text{int}} = \Delta H_{\text{cpx}} - (\Delta H_{\text{as}} + \Delta H_{\text{lig}}) \quad (2)$$

in which ΔH_{int} is the interaction enthalpy, ΔH_{cpx} is the heat of formation of the complex formed by the ligand and the enzyme model, ΔH_{as} is the heat of formation of the active site model, and ΔH_{lig} is the ligand heat of formation, both in the same conformations obtained in the energy minimized complex.

4.4. Empirical free energy model

Factors other than the interaction enthalpy may play important roles in the ligand-binding phenomenon. In a study of phorbol esters as inhibitors of protein kinase C, Wang et al.[34] have combined calculated interaction enthalpies, solubility, and entropy considerations in a thermodynamic cycle that allowed the prediction of free energies of binding, which correlated very well with measured binding constants. Based on a similar cycle, we developed an optimum free energy semiempirical model,

$$RT \ln K_{\text{i}} = c_1(\Delta G_{\text{solv}} + c_2)^n + c_3 \Delta H_{\text{int}} + c_4 N_{\text{RB}} + c_5 \quad (3)$$

K_{i} values were calculated from the IC_{50} data[36,63] and from $K_{\text{m}} = 1.6$ μM. The ΔG_{solv} solvation energy terms were determined by means of the SM5.4 model of Cramer and Truhlar.[64] The value of n (1 or 2) of the polynomial solvation energy term was adjusted tentatively. The ΔH_{int} terms were calculated by means of the PM3 semiempirical approach, as discussed previously (Eq. 2). In this work, as proposed previously by Wang et al.,[34] the N_{RB} term is the number of the ligand rotatable bonds that were frozen as a result of the ligand interaction with the atoms of the active site. By applying a multiple regression to develop an optimum model, we obtained the coefficients c_1–c_5 by fitting Eq. 3 to the experimental $\ln K_{\text{i}}$ values.

Acknowledgments

The Brazilian National Council of Research (CNPq) and the FAPERJ Foundation have supported this work. Contract Grant Nos. E26/150.711/2003, E26/171.199/2003, E26/171.401/01, E26/170.648/2004 and CNPq/IM-INOFAR 420.015/2005-1.

References and notes

1. Conti, M.; Jin, S. L. C. *Prog. Nucleic Acid Res. Mol. Biol.* **1999**, *63*, 1–38.
2. Houslay, M. D.; Sullivan, M.; Bolger, G. B. *Adv. Pharmacol.* **1998**, *44*, 225–342.
3. Huai, Q.; Wang, H.; Sun, Y.; Kim, H. Y.; Liu, Y.; Ke, H. *Structure* **2003**, *11*, 865–873.
4. Torphy, T. J. *Am. J. Respir. Crit. Care Med.* **1998**, *157*, 351–370.
5. Torphy, T. J.; Stadel, J. M.; Burman, M.; Cieslinski, L. B.; McLaughlin, M. M.; White, J. R.; Livi, G. P. *J. Biol. Chem.* **1992**, *267*, 1798–1804.
6. Jacobitz, S.; McLaughlin, M. M.; Livi, G. P.; Burman, M.; Torphy, T. J. *Mol. Pharmacol.* **1996**, *50*, 891–899.
7. Owens, R. J.; Catterall, C.; Batty, D.; Jappy, J.; Russell, A.; Smith, B.; O'Connell, J.; Perry, M. J. *Biochem. J.* **1997**, *326*, 53–60.
8. Rocque, W. J.; Tian, G.; Wiseman, J. S.; Holmes, W. D.; Zajac-Thompson, I.; Willard, D. H.; Patel, I. R.; Wisely, B.; Clay, W. C.; Kadwell, S. H.; Hoffman, C. R.; Luther, M. Z. *Biochemistry* **1997**, *36*, 14250–14261.
9. Carpenter, D. O.; Briggs, D. B.; Knox, A. P.; Strominger, N. *J. Neurophys.* **1988**, *59*, 358–369.
10. Eben, E.; Rüther, E. *Pharmacopsychiatry* **1985**, *18*, 69–70.
11. Horowski, R.; Sastre-y-Hernandez, M. *Curr. Ther. Res.* **1985**, *38*, 23–29.
12. Wxkman, F.; Fichte, K.; Meya, U.; Sastre-y-Hernandez, M. *Curr. Ther. Res.* **1988**, *43*, 195–291.
13. Wachtel, H. *Neuropharmacology* **1983**, *22*, 267–272.
14. Zeller, E.; Stief, H.-J.; Pflug, B.; Sastre-y-Hernandez, M. *Pharmacopsychiatry* **1984**, *17*, 188–190.
15. Sette, C.; Conti, M. *J. Biol. Chem.* **1996**, *271*(28), 16526–16534.
16. Alvarez, R.; Sette, C.; Yang, D.; Eglen, R. M.; Wilhelm, R.; Shelton, E. R.; Conti, M. *Mol. Pharmacol.* **1995**, *48*, 616–622.
17. Huston, E.; Pooley, L.; Julien, P.; Scotland, G.; McPhee, I.; Sullivan, M.; Bolger, G.; Houslay, M. *J. Biol. Chem.* **1997**, *271*, 31334–31344.
18. Xu, R. X.; Hassel, A. M.; Vanderwall, S.; Lambert, M. H.; Holmes, W. D.; Luther, M. A.; Rocque, W. J.; Milburn, M. V.; Zharo, Y.; Ke, H.; Nolte, R. T. *Science* **2000**, *288*, 1822–1825.
19. Xu, R. X.; Rocque, W. J.; Lambert, M. H.; Vanderwall, D. E.; Luther, M. A.; Nolte, R. T. *J. Mol. Biol.* **2004**, *337*, 355–365.
20. Laliberté, F.; Han, Y.; Govindarajan, A.; Giroux, A.; Liu, S.; Bobechko, B.; Lario, P.; Bartlett, A.; Gorseth, E.; Gresser, M.; Huang, Z. *Biochemistry* **2000**, *39*, 6449–6458.
21. Liu, S.; Laliberté, F.; Bobechko, B.; Bartlett, A.; Lario, P.; Gorseth, E.; Van Hamme, J.; Gresser, M. J.; Huang, Z. *Biochemistry* **2001**, *40*, 10179–10186.
22. Wu, G.; Vieth, M. *J. Med. Chem.* **2004**, *47*, 3142–3148.
23. Alcaro, A.; Gasparrini, F.; Incani, O.; Medduci, S.; Misiti, D.; Pierini, M.; Villani, C. *J. Comput. Chem.* **2000**, *21*, 515–530.
24. Brooks, C. L., III; Karplus, M.; Pettitt, B. M.. In *Proteins: A Theoretical Perspective of Dynamics, Structure, and Thermodynamics. Advances in Chemical Physics*; John Wiley & Sons: New York, 1988; Vol. LXXI,.
25. VanGunsteren, W. F.; King, P. M.; Mark, A. E. *Q. Rev. Biophys.* **1994**, *27*(4), 435–481.
26. Hansson, T.; Marelius, J.; Åqvist, J. *J. Comput. Aided Mol. Des.* **1998**, *12*, 27–35.
27. Åqvist, J.; Luzhkov, V. B.; Brandsdal, B. O. *Acc. Chem. Res.* **2002**, *35*, 358–365.
28. Asi, A. M.; Rahman, N. A.; Merican, A. F. *J. Mol. Graphics Modell.* **2004**, *22*, 249–262.
29. Raha, K.; Merz, K. M., Jr. *J. Am. Chem. Soc.* **2004**, *126*, 1020–1021.
30. Böhm, H. J. *J. Comput. Aided Mol. Des.* **1994**, *8*, 243–256.
31. Rarey, M.; Kramer, B.; Lengauer, T.; Klebe, G. *J. Mol. Biol.* **1996**, *261*, 470–489.
32. Eldridge, M. D.; Murray, C. W.; Auton, T. R.; Paolini, G. V.; Mee, R. P. *J. Comput. Aided Mol. Des.* **1997**, *11*, 425–445.
33. Williams, D. H.; Westwell, M. S. *Chem. Soc. Rev.* **1998**, *27*, 57–63.
34. Wang, S.; Milne, G. W. A.; Nicklaus, M. C.; Marquez, V. E.; Lee, J.; Blumberg, P. M. *J. Med. Chem.* **1994**, *37*, 1326–1338.
35. Searle, M. S.; Williams, D. H.; Gerhard, U. *J. Am. Chem. Soc.* **1992**, *114*, 10697–10704; Searle, M. S.; Williams, D. H. *J. Am. Chem. Soc.* **1992**, *114*, 10690–10697.
36. Dal Piaz, V.; Giovannoni, M. P.; Castellana, C.; Palacios, J. M.; Beleta, J.; Doménech, T.; Segarra, V. *Eur. J. Med. Chem.* **1998**, *33*, 789–797.
37. Sinnokrot, M. A.; Valeev, E. F.; Sherrill, C. D. *J. Am. Chem. Soc.* **2002**, *124*, 10887–10893.
38. Mannargudi, S. S.; Sasidhar, Y. U.; Balaji, P. V. *Protein Sci.* **2004**, *13*, 2502–2514.
39. Fernandez-Alonso, M. C.; Cañada, F. J.; Jimenez-Barbero, J.; Cuevas, G. *J. Am. Chem. Soc.* **2005**, *127*, 7379–7386.
40. Sujatha, M. S.; Sasidhar, Y. U.; Balaji, P. V. *Biochemistry* **2005**, *44*, 8554–8562.
41. Tauer, T. P.; Sherrill, C. D. *J. Phys. Chem. A* **2005**, *109*, 10475–10478.
42. Saldou, N.; Obernolte, R.; Huber, A.; Baecker, P. A.; Wilhelm, R.; Alvarez, R.; Li, B.; Xia, L.; Callan, O.; Su, C.; Jarnagin, K.; Shelton, E. R. *Cell. Signal.* **1998**, *10*, 427–440.
43. Gratteri, P.; Bonaccini, C.; Milani, F. *J. Med. Chem.* **2005**, *48*, 1657–1665.
44. Houslay, M. D.; Schafer, P.; Zhang, K. Y. J. *Drug Discovery Today* **2005**, *10*, 1503–1519.
45. Garmer, D. R.; Gresh, N.; Roque, B. *Proteins* **1998**, *31*, 42–60.
46. Antony, J.; Piquemal, J. H.; Gresh, N. *J. Comput. Chem.* **2005**, *26*, 1131–1147.
47. Donchev, A. G.; Ozrin, V. D.; Subbotin, M. V.; Tarasov, O. V.; Tarasov, V. I. *Proc. Natl. Acad. Sci. U.S.A.* **2005**, *102*, 7829–7834.
48. Tait, A.; Luppi, A.; Hatzelmann, A.; Fossa, P.; Mosti, L. *Bioorg. Med. Chem.* **2005**, *13*, 1393–1402.
49. Card, G. L.; England, B. P.; Suzuki, Y.; Fong, D.; Powell, B.; Lee, B.; Luu, C.; Tabrizizad, M.; Gillette, S.; Ibrahim, P. N.; Artis, D. R.; Bollag, G.; Milburn, M. V.; Kim, S. H.; Schlessinger, J.; Zhang, K. Y. J. *Structure* **2004**, *12*, 2233–2247.
50. Berendsen, H. J. C.; Vanderspoel, D.; Vandrunen, R. *Comput. Phys. Commun.* **1995**, *91*, 43–56.
51. Lindahl, E.; Hess, B.; van der Spoel, D. *J. Mol. Model.* **2001**, *7*, 306–317.
52. Jorgensen, W. L.; Tirado-Rives, J. *J. Am. Chem. Soc.* **1988**, *110*, 1657–1666.
53. Jorgensen, W. L. J.; Chandrasekhar, J.; Madura, J. D.; Impey, R. W.; Klein, M. L. *J. Chem. Phys.* **1983**, *79*, 926–935.
54. Ryckaert, J. P.; Bellemans, A. *Faraday Discuss. Chem. Soc.* **1978**, *66*, 95–106.
55. Hess, B.; Bekker, H.; Berendsen, H. J. C.; Fraaije, J. G. E. M. *J. Comput. Chem.* **1997**, *18*, 1463–1472.
56. Hockney, R. W.; Goel, S. P.; Eastwood, J. W. *J. Comput. Phys.* **1974**, *14*, 148–158.

57. Morris, G. M.; Goddsell, D. S.; Halliday, R. S.; Huey, R.; Hart, W. E.; Belew, R. K.; Olson, A. J. *J. Comput. Chem.* **1998**, *19*, 1639–1662.
58. Halgren, T. *J. Comput. Chem.* **1996**, *17*, 490–519.
59. Sinnokrot, M. O.; Sherrill, C. D. *J. Chem. Phys. Chem. A* **2003**, *107*, 8377–8379.
60. Stewart, J. J. P. QCPE 455, available from Indiana University, Bloomington, USA, 1992.
61. Stewart, J. J. P. *J. Comput. Chem.* **1989**, *10*, 209–220; Stewart, J. J. P. *J. Comput. Chem.* **1989**, *10*, 221–264.
62. Baker, J. *J. Comput. Chem.* **1986**, *7*, 385–395.
63. Cheng, Y.; Prusoff, W. H. *Biochem. Pharm.* **1973**, *22*, 3099–3108.
64. Chambers, C. C.; Hawkins, G. D.; Cramer, C. J.; Truhlar, D. G. *J. Phys. Chem.* **1996**, *100*, 16385–16398.